



OPEN Evaluation method for public guidance service interface design based on improved grey H-Convex correlation model: integrating layout aesthetics and user visual cognition

Weiwei Wang¹✉, Zhiqiang Wen¹, Zhanmei Hu², Jian Chen¹, Yanhui Gu¹ & Qizhao Peng¹

The development of scientifically rigorous evaluation methods is essential to overcome three persistent challenges in public navigation interfaces: inadequate guidance, low usability, and suboptimal user experience. Focusing on intelligent medical guidance systems, this study establishes a dual-dimensional analytical framework encompassing layout aesthetics (spatial composition principles) and visual cognition (information processing patterns). We propose an enhanced grey H-convex correlation model integrating Bayesian Best Worst Method (BBWM) and modified CRITIC with reference point (M-CRITIC-RP) to address weight determination limitations in existing models. Our experimental analysis reveals two key findings: First, the synergistic integration of layout aesthetics (e.g., visual hierarchy balance) and visual cognition characteristics (e.g., attention distribution patterns) significantly improves interface usability for medical service navigation. Second, the proposed BBWM-M-CRITIC-RP hybrid model demonstrates superior performance in quantifying aesthetic-cognition relationships, achieving 88% prediction accuracy compared to conventional methods. In a word, our research provides a new theoretical method for traditional visual display design and a new evaluation criterion for interface design, aiming at improving the user experience.

Keywords Public guidance service interface, Layout aesthetics, Visual cognitive, Medical guidance desk, BBWM, M- CRITIC-RP, Grey H-convex correlation

The ongoing digital transformation has significantly deepened the integration between public services and information technologies¹. Within this context, public guidance interfaces-digital platforms enabling service access in urban environments-exhibit distinct interaction characteristics compared to personal devices like smartphones or vehicle dashboards. These systems follow an intermittent usage pattern: while daily engagement remains limited, users demand immediate task completion during critical service encounters². This operational paradigm creates three essential design requirements for public guidance interfaces deployed in healthcare facilities, transportation hubs, and cultural institutions (1) Visual salience to attract attention in crowded environments. (2) Zero-learning-curve operation for first-time users. (3) Time-constrained task efficiency for urgent service needs. Unlike high-frequency interfaces requiring habitual usage patterns, public guidance systems must achieve immediate usability without prior training while maintaining aesthetic appeal. This dual requirement of visual attractiveness and instant operational clarity defines their unique design challenges in public service scenarios.

Current public guidance interfaces suffer from three persistent design flaws: inadequate navigation cues, inefficient service delivery, and excessive operational complexity, collectively leading to suboptimal user experiences³. These shortcomings become particularly acute in healthcare settings where urgent service demands prevail⁴. As critical healthcare infrastructure, medical guidance desks must fulfill two essential functions: (1) providing immediate wayfinding solutions and (2) enabling rapid service acquisition for patients under time-

¹College of Design and Art, Shaanxi University of Science and Technology, Xian 710021, China. ²Shaanxi University of International Trade & Commerce, Xian 710021, China. ✉email: wangweiwei@sust.edu.cn

sensitive conditions. Current research identifies critical challenges in healthcare interface design. Suboptimal guidance systems have been shown to induce user confusion and frustration⁵, particularly detrimental in emergency care environments where overcrowding and prolonged wait times exacerbate patient dissatisfaction⁶. The complexity of patient journeys—spanning registration, triage, treatment, and discharge—creates cumulative interaction barriers that challenge service quality maintenance⁷. Meanwhile, bedside clinical decision support (CDS) systems demonstrate the operational advantages of minimizing physician reliance on spatially distant desktop interfaces⁸. These findings collectively underscore the pressing need for interface designs that balance visual salience with operational immediacy in healthcare navigation systems.

This investigation establishes a dual-criteria evaluation framework for hospital guidance interfaces, systematically incorporating both aesthetic perception (spatial composition principles) and visual cognition patterns (information processing mechanisms). The proposed methodology generates actionable design guidelines to optimize medical navigation systems through enhanced interface intuitiveness and user-centric information architecture. These improvements directly target two operational objectives: (1) accelerating users' task completion efficiency and (2) reducing dependency on staff-assisted navigation services.

Literature review

Visual interface design

Visual design quality evaluation operates through three interconnected dimensions: aesthetic perception, functional efficiency, and symbolic representation, each grounded in distinct theoretical foundations⁹. The aesthetic dimension traces its conceptual origin to Alexander Baumgarten's 1750 treatise *Aesthetica*, which formalized aesthetics as the scientific study of sensory cognition (Greek: *aisthētikos*), positing aesthetics as the optimal realization of perceptual awareness¹⁰. This theoretical framework explains how interface aesthetics govern user perception dynamics, as evidenced by Sulikowski et al.'s eye-tracking studies revealing aesthetic features' influence on visual attention allocation¹¹.

Functional evaluation employs interaction laws like Fitts' Law¹² - a mathematical model quantifying target acquisition time as a function of element size and movement distance - to assess interface operational efficiency. Meanwhile, the symbolic dimension incorporates cultural semantics and identity communication mechanisms, with Lee et al.¹³ and Lidwell et al.¹⁴ developing universal design principles for interface application scenarios through cognitive psychology theories and empirical case syntheses.

Aesthetics and functionality, as critical aspects of visual design for infrequently used interfaces, have garnered extensive academic attention. Research has primarily focused on aesthetic perception, aesthetic measurement, and human cognitive characteristics, yielding notable advancements. However, existing studies often fail to integrate these dimensions, potentially leading to discrepancies between interface design quality and actual user needs. On the one hand, aesthetics significantly influence visual design in unconventional public-oriented service interfaces. Visually appealing interfaces enhance user engagement. Scholars have explored user experience and usability by investigating intrinsic properties of design elements, including icons¹⁵, layouts¹⁶, and typography¹⁷. Research also addresses subjective dimensions like visual complexity¹⁸, utility¹⁹, and attractiveness²⁰. Birkhoff (1933) proposed a seminal mathematical formula for macro-aesthetics: $M = O/C$, defining aesthetic measure as the order-complexity ratio²¹. Ngo et al. developed computational aesthetic models to quantify layout characteristics in interface design²².

On the other hand, visual perception serves as the primary channel for information perception in human interactions with infrequently used interfaces²³. Integrating human cognitive features into interface design ensures alignment with user mental models, which is critical for effective interaction. Researchers have evaluated interface design through visual cognition theories. For instance, Zhi et al.²⁴ analyzed layout types in train cockpit interfaces using eye-tracking experiments to assess visual cognitive load, search efficiency, and attention distribution. Similarly, Martinez et al.²⁵ examined cockpit dashboard interfaces by analyzing pilots' gaze patterns and visual cognition via eye-tracking metrics, focusing on gaze trajectories, fixation distribution, and frequency to minimize operational errors.

In summary, significant progress has been made in interface design evaluation, yet existing research predominantly focuses on frequently used interfaces, with limited attention to infrequently used systems such as medical guidance interfaces. Current studies often examine layout aesthetics or visual cognition in isolation, neglecting their combined influence, which risks incomplete assessments of design quality. Notably, quantitative investigations into the mapping relationships between interface layout aesthetics and visual cognitive features remain scarce.

Grey correlation analysis

The evaluation of public service guidance interface layouts can be conceptualized as a "grey system," where aesthetic metrics and visual cognitive physiological measurements represent "white systems," while their coupling relationships form an unknown "black system." Grey theory excels in addressing uncertainties with partial information availability. Grey relational analysis, a core component of grey system theory, evaluates relational degrees based on geometric similarities of data sequence curves²⁶. Existing models include the grey entropy correlation model²⁷, grey B-type relational model²⁸, and new grey absolute relational model²⁹.

However, traditional grey correlation methods are limited to positive correlations and fail to capture negative relationships. To resolve this, Wu et al.³⁰ proposed a grey convex correlation model that measures sequence convexity via vertical distances. Pan et al.³¹ introduced the grey H-convex relational degree using span and arch height principles to quantify negative correlations through horizontal convexity. Recent advancements extend these methods to three-dimensional panel data, exemplified by Dang et al.'s³² grey vector relational model based on 3D geometric features, addressing comparability in multi-dimensional data analysis.

While existing models have advanced significantly, they retain notable limitations. For instance, the assessment of sequence curve similarity often overlooks indicator weighting or relies on oversimplified or ambiguous weighting methods, introducing deviations from actual outcomes.

Weighting method

Existing studies divide weight determination methods into two categories: subjective and objective.

(1) Subjective methods rely on expert knowledge and experience to assign criterion weights. For example, Liu et al.³³ applied the Analytic Hierarchy Process (AHP) to calculate weights for interface evaluation criteria, proposing a human-machine interface reliability evaluation framework. Vrtađić et al.³⁴ employed the Step-wise Weight Assessment Ratio Analysis (SWARA) to assess weight coefficients for enhancing traffic route safety. Gul et al.³⁵ (2022) utilized the Bayesian Best-Worst Method (BBWM) to prioritize criteria for assessing safety risks in specific environments.

(2) Objective methods employ mathematical techniques based on inter-criteria relationships within raw data, eliminating human subjectivity. Examples include the entropy weight method, Criteria Importance Through Intercriteria Correlation (CRITIC), and M-CRITIC-RP. Chen et al.³⁶ integrated entropy weighting to evaluate product conceptual design. Sharkasi et al.³⁷ applied M-CRITIC-RP to compute multi-criteria weights, combined with a gravity model to analyze product export potential. Neither approach fully captures all criteria information. Thus, hybrid methods—such as least squares³⁸ and game theory-based approaches³⁹—combine subjective and objective weighting to achieve balanced results.

BBWM

The Best-Worst Method (BWM), initially proposed by Rezaei et al., deviates from pairwise comparisons by focusing on identifying the most and least important criteria and evaluating their priority relative to others⁴⁰. However, BWM is limited to individual decision-maker judgments. To address this, Mohammadi et al.⁴¹ developed the Bayesian Best-Worst Method (BBWM), which treats criteria as probabilistic events, with weights represented as occurrence probabilities. BBWM processes BWM inputs via multinomial distributions and calculates criterion weights using Dirichlet distributions. By constructing a Bayesian framework, BBWM derives optimal weights reflecting collective preferences across multiple decision-makers.

M-CRITIC-RP

The Criteria Importance Through Intercriteria Correlation (CRITIC) method faces two key limitations: (1) Its data normalization process requires categorizing criteria into strictly positive or negative attributes, leading to distortions when criteria do not strictly fit these categories. (2) Its reliance on Pearson correlation coefficients restricts weight calculation to linear relationships, ignoring nonlinear interdependencies.

To resolve these issues, Sharkasi et al.⁴² proposed the M-CRITIC-RP method, which employs fuzzy logic theory and Hamming distance to optimize normalization and mitigate rigid positive/negative attribute categorization. Additionally, distance correlation coefficients replace Pearson correlations to construct weighting matrices, enabling detection of both linear and nonlinear relationships.

Motivation

Existing research reveals limited exploration of evaluation methods for infrequently used interfaces, sparse integration of interface layout aesthetics with visual cognition, and minimal investigation into their interrelationships. Consequently, the proposed method demonstrates significant application potential in addressing these gaps.

In a previous study, we developed a grey H-convex relational model for the virtual museum interface using the Improving Criteria Importance through Inter-Criteria Correlation (ICRITIC) methodology⁴³, which did not take into account subjective criterion weights. This work advances this framework through key method innovation: using BBWM and M-Critical-RP methods to determine the subjective and objective weights of indicators, and introducing game theory model to realize the dynamic balance between subjective and objective weights, thus improving the applicability of the model in the medical guidance interface.

To enhance the accuracy of mapping interface layout aesthetics to visual cognition, we introduced a weight determination step. BBWM and M-CRITIC-RP were selected due to their superiority over alternative weighting methods. Additionally, the grey H-convex relational model outperforms conventional grey models in handling nonlinear relationships, as demonstrated in subsequent comparative analyses.

Research framework

The framework is structured as follows (Fig. 1). First, an evaluation criteria system for human-machine interface layouts is established through emotional imagery analysis and literature review, followed by metric data generation. Next, comprehensive criterion weights are computed using BBWM (subjective weights), M-CRITIC-RP (objective weights), and a game-theoretic equilibrium model to unify both weight types. Weighted normalization is then applied to standardize input data for the grey H-convex relational model, which quantifies correlations between layout aesthetics and visual cognition.

Methods

Evaluation criteria

The evaluation criteria system for human-machine interface layouts comprises two components: interface layout aesthetics criteria and visual cognition evaluation criteria. Firstly, this study adopted a three-phase stratified validation protocol involving expert, professional, and non-professional groups with distinct roles. (1) Expert panel: To validate the evaluation system, comprising 4 human-computer interaction design professors and 2

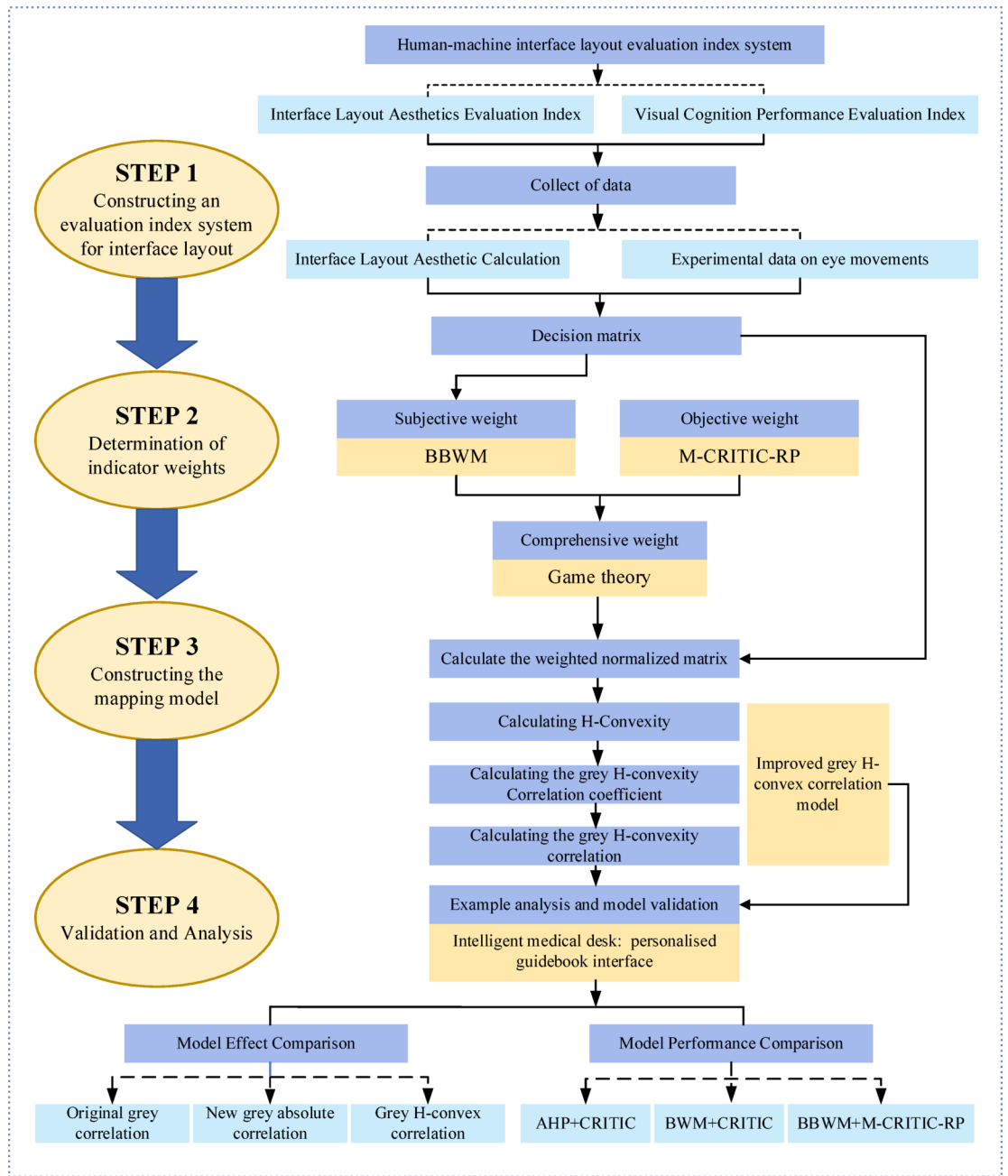


Fig. 1. Research framework.

chief information officers from tertiary hospitals. (2) Aligned with Nielsen’s parallel design theory⁴⁴, consisting of trained designers (with interaction design expertise and medical interface project experience) for precise decomposition of layout aesthetic. (3) Non-professional group ($n = 15$): Representing end-users. A minimum sample size ($n = 12$) was determined via G-Power 3 ($\alpha = 0.05, \beta = 0.2, \text{effect size} = 0.4$). Inclusion criteria: at least 2 visits to tertiary hospitals in the past 6 months⁴⁵. Secondly, 26 smart medical console interface prototypes were designed following interface design principles. The professional group conducted emotional imagery analysis on the prototypes, which were then evaluated and refined by the non-professional group. This process yielded 16 distinct imagery descriptors through preliminary screening based on semantic divergence. The non-professional group subsequently assessed the prototypes using a 7-point Likert scale. Structural validity of the questionnaire was confirmed via Exploratory Factor Analysis (EFA) ($KMO = 0.82$, Bartlett’s sphericity test $p < 0.001$), with five factors accounting for 91.3% cumulative variance. Reliability testing using Cronbach’s alpha demonstrated strong internal consistency ($\alpha = 0.87$; all factor-specific $\alpha > 0.7$). Five layout aesthetic criteria were ultimately selected: Balance, Density, Simplicity, Order, and Uniformity.

On the other hand, existing research indicates that interface element layout significantly influences users’ visual cognitive performance⁴⁶. Five validated eye-tracking metrics linked to interface layout aesthetics include

gaze duration⁴⁷, gaze count⁴⁸, mean pupil diameter⁴⁹, saccadic frequency⁵⁰, and fixation time percentage⁵¹. These metrics were selected as evaluation criteria for public service-oriented interface design. The human-machine interface layout evaluation framework is depicted in Fig. 2.

Evaluation model

Model frame

The model framework is divided into three parts, as shown in Fig. 3.

(1) Collecting data. On one hand, aesthetic evaluation values were obtained based on formulas. On the other hand, user visual cognitive characteristics were derived from eye-tracking experiments. Let the interface layout aesthetics evaluation criteria be $\{C_1^a, C_2^a, C_3^a \cdots, C_n^a\}$, the eye movement criteria is $\{C_1^e, C_2^e, C_3^e \cdots, C_n^e\}$.

(2) Weight distribution. The BBWM method determines subjective weights, while the M-CRITIC-RP method calculates objective weights. Finally, using the principles of game theory, the standard combination weights were determined.

(3) Construct an improved grey H-convex correlation model. Establish a weighted standardized indicator data sequence as input for the model. Using the grey H-convex correlation method, quantitatively evaluate the correlation between eye movement indicators and layout aesthetics indicators.

Data collection

(1) Layout aesthetics value.

Building on the shape superiority effect in cognitive processing psychology, interface layout elements were functionally zoned and abstracted into black rectangles to achieve precise positioning⁵². A coordinate system was established to compute layout aesthetic metrics (Fig. 4), with four parameters defining spatial positioning: the horizontal coordinate x , the vertical coordinate y , the total width b and the total height h of the rectangle. Overall layout dimensions: $b \times h = 400 \times 300$ mm. Among them, along the interface from left to right is the x -positive direction, and from top to bottom scanning is the y -positive direction. According to aesthetic calculation formula proposed by Ngo et al.²², calculate the evaluation results of aesthetics indicators.

1) Balance C_1^a

The degree of balance indicates the symmetry of the elements in the interface layout in three directions: vertical, horizontal and diagonal. It is calculated by the formula²².

2) Intensity C_2^a

Intensity represents the tightness or looseness of the elements in the interface. An optimal interface intensity is achieved at 50%²².

3) Simplicity C_3^a

Simplicity refers to the degree of element arrangement and integration in an interface layout to reduce users' cognitive load in perceiving layout configurations²².

4) Order C_4^a

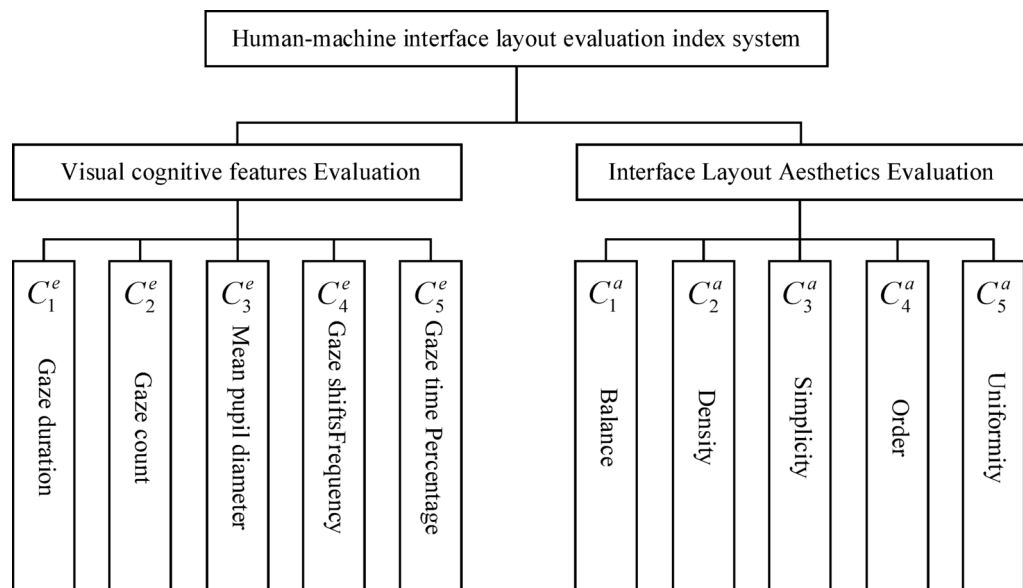


Fig. 2. Evaluation criteria system of human-machine interface layout.

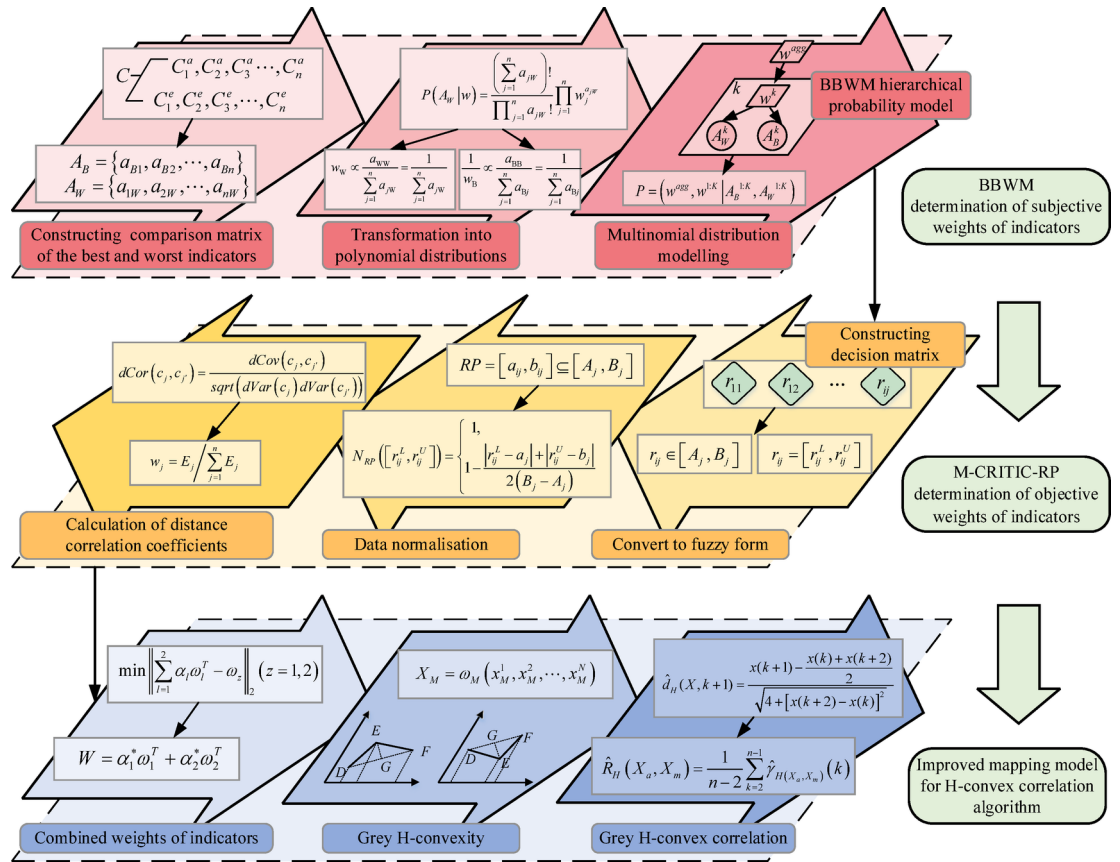


Fig. 3. Model framework.

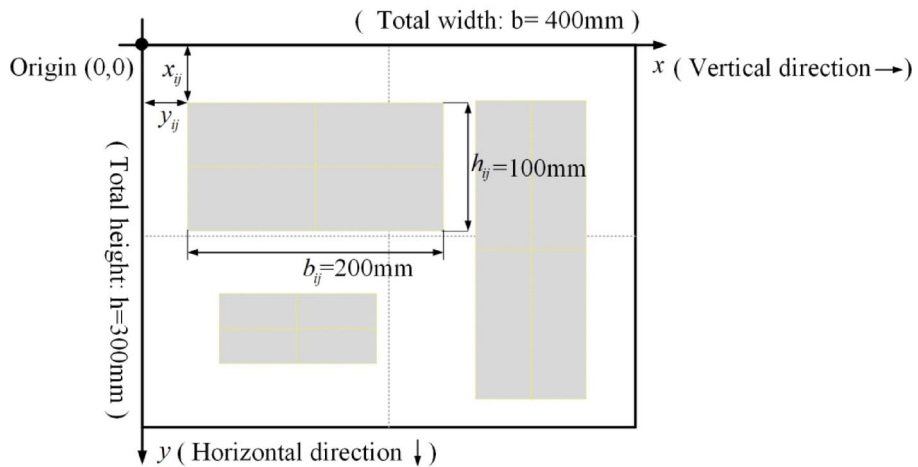


Fig. 4. Coordinate system for interface layout aesthetics calculation. Origin (0,0) at top-left corner with x-axis positive to the right, y-axis positive downward. Interface elements are abstracted as black rectangles parameterized by position (x_{ij}, y_{ij}) and dimensions (b_{ij}, h_{ij}) .

The human eye has reading habits from top to bottom, from left to right, from large objects. The interface layout according to this visual law can effectively guide the order of human attention²².

5) Uniformity C_5^a

Uniformity emphasizes the visual coherence of interface layout elements. It is usually calculated as the aspect ratio of the interface layout elements to the interface frame²².

(2) Visual Cognition Measurement.

Eye-tracking technology enables the acquisition of physiological data on visual cognition by observing interface element layouts and capturing variations in user gaze trajectories. The sample size of 42 participants was determined via a priori power analysis using G-Power 3.1, which indicated a minimum requirement of 38 subjects to detect a medium effect size ($f^2=0.25$) with 95% power for multiple regression analysis involving five predictors at $\alpha=0.05$. This exceeds the recommended threshold in interface eye-tracking studies⁵³. Participants underwent rigorous screening including: 1) Questionnaire-based exclusion of prior eye-tracking experience. 2) Gender-balanced recruitment (21 males/21 females). 3) Age stratification (24–55 years) ensured representation of key medical kiosk user demographics, with screening intentionally excluding individuals under 24 (infrequent users) and over 55. All participants had normal or corrected-to-normal vision in both eyes and were free from color vision deficiencies.

The subjects were seated in a fixed position, with the eye distance to the front of the monitor maintained at 60.2 ± 3.1 cm (mean \pm SD) through postural adjustments. The experimental equipment was a Tobii X2-30 eye-tracker with a sampling frequency of 30 Hz, coupled with a 21.5-inch Hewlett-Packard desktop monitor, featuring a screen resolution of 1920×1080 PX. The experimental program was written and run with the help of ErgoLAB, designed for the acquisition of experimental data. The experiment utilized flicker-free LEDs ($5500 \text{ K} \pm 5\%$ color temperature) with stable illumination of 250 ± 10 lx (calibrated by Testo 540 light meter) to ensure environmental consistency for pupillometry. All participants underwent a 9-point eye tracker calibration procedure, achieving a mean error of $<0.5^\circ$, thereby guaranteeing measurement accuracy.

Criteria weights

(1) Subjective weighting.

The subjective weights are calculated based on BBWM.

Step.1 Identification of a collection of evaluation criteria $C = \{C_1, C_2, \dots, C_n\}$.

Step.2 Experts based on industry information, actual investigation and subjective experience from the interface layout evaluation system $C = \{C_1, C_2, \dots, C_n\}$ initially determine the best C_B and worst C_W criteria as reference and comparison object.

Step.3 Constructing comparison guidelines. Experts compare C_B with other interface layout evaluation indicators in pairs to obtain a matrix: $A_B = \{a_{B1}, a_{B2}, \dots, a_{Bn}\}$. Among them, a_{Bj} represents the ratio of the importance of C_B to other interface layout evaluation indicators, expressed as integers ranging from 1 to 9, and $a_{BB}=1$. Similarly, by comparing other interface layout evaluation indicators with C_W in pairs, a matrix is obtained: $A_W = \{a_{1W}, a_{2W}, \dots, a_{nW}\}$. Among them, a_{iW} represents the ratio of the importance of other interface layout evaluation indicators to C_W , expressed as integers ranging from 1 to 9, with $a_{WW}=1$.

Step.4 Introduce polynomial distribution and Dirichlet distribution as the probability distribution assumptions for the input and output of BBWM model.

Step.5 Transform the weight judgment problem of interface layout evaluation indicators into a probability statistical problem of approximating the posterior distribution of the best weight vector, and calculate the best weight vector w^{agg} for group decision-making.

Considering the joint influence of A_B and A_W the optimal weight vector for evaluating the layout of public guidance service interfaces in expert group decision-making is calculated based on a Bayesian hierarchical model. Setting with k^{th} experts, $k = 1, \dots, K$, determines the best and worst comparison matrices A_W^k and A_B^k based on the interface layout evaluation criteria C_1, \dots, C_n , the set of best and worst-case comparison matrices for the k experts is $A_B^{1:K}$ and $A_W^{1:K}$. Let w^{agg} denote the optimal weight vector for expert group decision-making, calculated based on the optimal weight vector w^k ($k = 1, \dots, K$) for each expert. Before calculating the w^{agg} , the joint probability distribution of the evaluation random variables for the public guidance service interface should be represented based on the given parameters. $A_B^{1:K}$ and $A_W^{1:K}$ are given, while w^{agg} and $w^{1:K}$ are the quantities that need to be solved. Therefore, the joint probability distribution of w^{agg} can be expressed as:

$$P(w^{agg}, w^{1:K} | A_B^{1:K}, A_W^{1:K}) \quad (1)$$

In the Bayesian hierarchical model, $w^{1:K}$ is both the variable to be solved and the parameter to solve w^{agg} . According to the chain rule, Eq. (1) is represented as:

$$\begin{aligned} & P(w^{agg}, w^{1:K} | A_B^{1:K}, A_W^{1:K}) \\ & \propto P(A_B^{1:K}, A_W^{1:K} | w^{agg}, w^{1:K}) P(w^{agg}, w^{1:K}) \\ & = P(w^{agg}) \prod_{k=1}^K P(A_W^k | w^k) P(A_B^k | w^k) P(w^k | w^{agg}). \end{aligned} \quad (2)$$

Where $P(w^{agg}, w^{1:K} | A_B^{1:K}, A_W^{1:K})$ represents the posterior distribution of w^{agg} , $P(w^{agg})$ represents the prior distribution of w^{agg} , $P(A_W^k | w^k)$ and $P(A_B^k | w^k)$ represents the polynomial distribution assumption of A_W^k and A_B^k , $P(w^k | w^{agg})$ represents the prior distribution of w^k .

The process of solving the posterior distribution of w^{agg} and w^k involves high-dimensional integration, which is difficult to calculate. Therefore, using the Markov chain Monte Carlo method in Gibbs sampling environment, fitting the posterior distributions of w^{agg} and w^k , and finally taking the sample mean of the w^{agg} posterior distribution as the optimal weight result.

(2) Objective weighting.

The M-CRITIC-RP method calculates the objective weights of interface layout evaluation criteria.

(1) Define the decision matrix R . With m interface programs and n criteria, there are,

$$R=(r_{ij})_{m \times n}; i = 1, \dots, m; j = 1, \dots, n \tag{3}$$

Where r_{ij} represents the elements of the decision matrix for the j criteria in the i interface program.

(2) The clear values of the decision matrix elements $r_{ij} \in [A_j, B_j]$ are transformed into the fuzzy form $[r_{ij}^L, r_{ij}^U]$.

(3) Specify the fuzzy reference point RP for each standard c_j . The fuzzy RP points are $[a_{ij}, b_{ij}] \subseteq [A_j, B_j]$, where $a_{ij} = \sum_{i=1}^m r_{ij}^L / m; b_{ij} = \sum_{i=1}^m r_{ij}^U / m$ is the mean of r_{ij}^L and r_{ij}^U , fuzzy element $r_{ij}^L = r_{ij} - h_i, r_{ij}^U = r_{ij} + h_i, h_i$ is some positive decimal, for all i and j : $0 < r_{ij} + h_i < 1, 0 < r_{ij} - h_i < 1$. Besides, $A_j = \min_i r_{ij}^L, B_j = \max_i r_{ij}^U$.

(4) The decision matrix is normalized and the calculation is expressed as follows

$$N_{RP}([r_{ij}^L, r_{ij}^U]) = \begin{cases} 1, & [r_{ij}^L, r_{ij}^U] \subseteq [a_j, b_j] \\ 1 - \frac{|r_{ij}^L - a_j| + |r_{ij}^U - b_j|}{2(B_j - A_j)}, & [r_{ij}^L, r_{ij}^U] \not\subseteq [a_j, b_j], [r_{ij}^L, r_{ij}^U] \subseteq [A_j, B_j] \end{cases} \tag{4}$$

(5) Calculate the standard deviation S_j of the j interface evaluation criteria.

$$S_j = \sqrt{\frac{(\sum_{i=1}^m x_{ij} - \bar{x}_j)^2}{m - 1}} \tag{5}$$

(6) Calculation of distance correlation coefficients $dCor(c_j, c_{j'})$.

$$dCor(c_j, c_{j'}) = \frac{dCov(c_j, c_{j'})}{\sqrt{dVar(c_j) dVar(c_{j'})}} \tag{6}$$

Where $dCov(c_j, c_{j'})$ denotes the distance covariance of c_j and $c_{j'}, dVar(c_j) = dCov(c_j, c_j)$ denotes the distance variance of $c_j, dVar(c_{j'}) = dCov(c_{j'}, c_{j'})$ denotes the distance variance of $c_{j'}$.

(7) Calculation of the amount of information E_j .

$$E_j = S_j \sum_{j=1}^n (1 - dCor(c_j, c_{j'})) \tag{7}$$

(8) Calculation of the weighting factor w_j .

$$w_j = \frac{E_j}{\sum_{j=1}^n E_j} \quad j = 1, 2, \dots, n \tag{8}$$

(3) Combined weights.

By applying game theory principles, this study adopts the attainment of Nash equilibrium⁵⁴ as the optimization goal for harmonizing subjective and objective weights. The objective is to identify an equilibrium point that minimizes deviations between the integrated weights and the original base weights, thereby deriving optimal composite weights.

Step.1 There are E different weighting methods to assign weights $W_z = \{\omega_{z1}, \omega_{z2}, \dots, \omega_{zn}\} (z = 1, 2, \dots, L)$, where ω_{zj} denotes the weight of interface layout criteria j under weighting method z , This paper $L = 2$. Let $\alpha = \{\alpha_1, \alpha_2\}$ be a linear combination of coefficients, then:

$$W = \alpha_1 \omega_1^T + \alpha_2 \omega_2^T (\alpha_{1,2} > 0, \alpha_1 + \alpha_2 = 1) \tag{9}$$

Step.2 Introducing the idea of game-theoretic aggregation model, the optimal weights W are obtained with the objective of minimizing the deviation between W and W_k . The objective function is:

$$\min \left\| \sum_{l=1}^2 \alpha_l \omega_l^T - \omega_z \right\|_2 \quad (z = 1, 2) \tag{10}$$

According to the differential characteristics of the matrix, the optimal first-order derivative conditional equation of Eq. (10) is as follows:

$$\begin{bmatrix} \omega_1 \cdot \omega_1^T & \omega_1 \cdot \omega_2^T \\ \omega_2 \cdot \omega_1^T & \omega_2 \cdot \omega_2^T \end{bmatrix} \times \begin{bmatrix} \alpha_1 \\ \alpha_2 \end{bmatrix} = \begin{bmatrix} \omega_1 \cdot \omega_1^T \\ \omega_2 \cdot \omega_2^T \end{bmatrix} \tag{11}$$

Step.3 Normalizing the optimized combination coefficients $\alpha = \{\alpha_1, \alpha_2\}$.

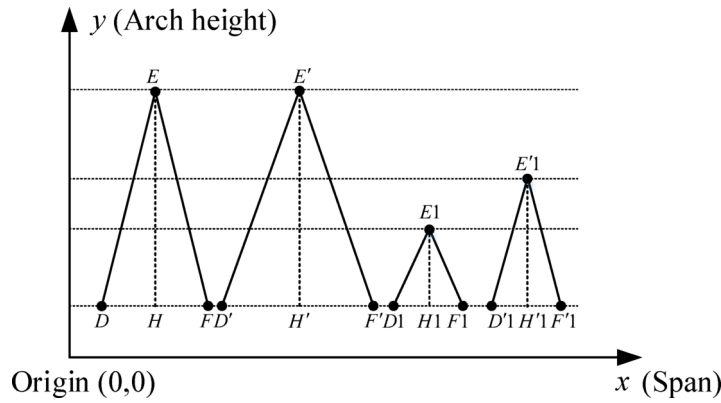


Fig. 5. Schematic of H-convex correlation with bridge-inspired span-arch principles. Coordinate system: X-axis (Span), Y-axis (Arch height). The figure presents a schematic representation of four folds with different spans and arch heights.

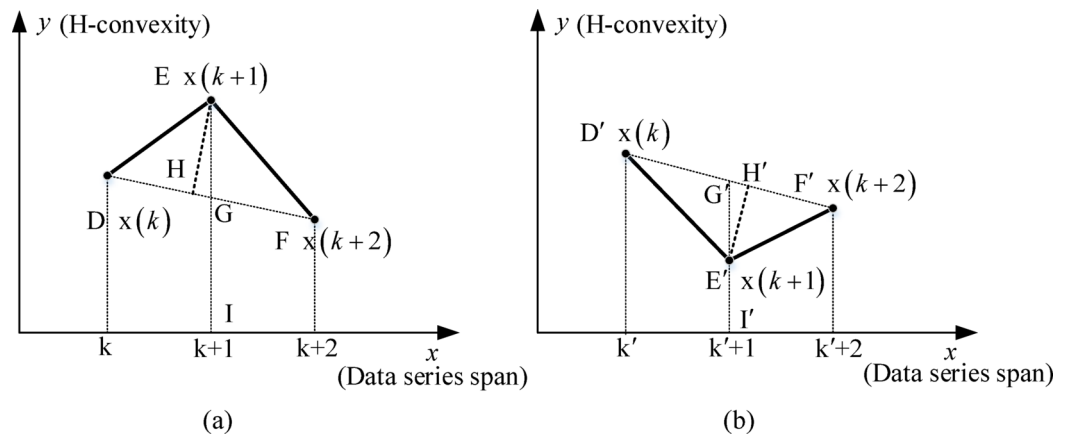


Fig. 6. Schematic calculation of H-convexity. Figure 6-(a), Fig. 6-(b) shows the two cases of H-convexity calculation respectively. The X-axis represents the data series span and the Y-axis represents the H-convexity. Solid line folds show the change in convexity for three consecutive data (k, k + 1, k + 2).

$$\alpha_z^* = \frac{|\alpha_z|}{\sum_{z=1}^2 |\alpha_z|} \tag{12}$$

Step.4 Calculate the combined weights W .

$$W = \alpha_1^* \omega_1^T + \alpha_2^* \omega_2^T \tag{13}$$

Improved grey H-convex correlation model

The grey H-convex relational model applies principles of span and arch height from bridge engineering to characterize the horizontal convexity of polyline curves³¹. Crucially, it distinguishes both positive and negative correlations between data sequences.

Definition 1 As shown in Fig. 5, for a fold line DEF , the line segment DF denotes the span.

Definition 2 As shown in Fig. 5, for a broken line DEF , the vertical line HE between the vertex E and the span DF represents the height of the arch.

Definition 3 As shown in Fig. 6, for any concave-convex folding line DEF , arch height HE , spans DF . Then the ratio $\frac{HE}{DF}$ of the arch height HE to the span DF is the H-convexity of the fold DEF , expressed as $d_{H-convex} = \frac{HE}{DF}$.

As shown in Fig. 6, based on $x(k), x(k+1), x(k+2)$ in the interface evaluation criteria series X plotting the fold DEF , $\text{spans}DF = \sqrt{(k+2-k)^2 + [x(k+2) - x(k)]^2} = \sqrt{4 + [x(k+2) - x(k)]^2}$, for ease of calculation, the value of GE is used instead of the arch height $HE, GE = x(k+1) - \frac{x(k)+x(k+2)}{2}$, then the H-convexity of the sequence X at $t = k + 1$ is recorded as $\hat{d}_H(X, k + 1)$,

$$\hat{d}_H(X, k + 1) = \frac{x(k + 1) - \frac{x(k)+x(k+2)}{2}}{\sqrt{4 + [x(k + 2) - x(k)]^2}} \tag{14}$$

Definition 4 Let the interface layout evaluation criteria M , and the interface N , x_m^n is the value of interface layout evaluation for the n ($n = 1, 2, \dots, N$) interface of criteria m , Set ω_i as the comprehensive weight of the i -th index. The weighted normalized data series form m criteria is then expressed as, $X_a = \omega_a (x_a^1, x_a^2, \dots, x_a^N)$, $X_b = \omega_b (x_b^1, x_b^2, \dots, x_b^N)$, \dots , $X_M = \omega_M (x_M^1, x_M^2, \dots, x_M^N)$. Then the grey H-convexity coefficients of X_a and X_m at $t = k$ is,

$$\hat{\gamma}_{H(X_a, X_m)}(k) = \text{sgn}(\hat{d}_H(X_a, k), \hat{d}_H(X_m, k)) \frac{1}{1 + ||\hat{d}_H(X_a, k) - \hat{d}_H(X_m, k)||} \tag{15}$$

For weighted normalized data series $X_a = \omega_a (x_a^1, x_a^2, \dots, x_a^N)$, $X_b = \omega_b (x_b^1, x_b^2, \dots, x_b^N)$, \dots , $X_M = \omega_M (x_M^1, x_M^2, \dots, x_M^N)$, The grey H-convex correlation between sequences X_a and X_m is denoted by $\hat{R}_H(X_a, X_m)$, abbreviated as $\hat{R}_H(a, m)$, then,

$$\hat{R}_H(a, m) = \frac{1}{n-2} \sum_{k=2}^{n-1} \hat{\gamma}_{H(X_a, X_m)}(k) \tag{16}$$

Application

The primary function of the guide desk is to provide convenient, accurate and friendly medical guidance and services to patients. The system provides personalized guidance processes based on each patient’s condition and treatment plan, including registration, diagnosis and treatment, examination, and guidance.

Samples

Using clustering analysis, 10 interface samples exhibiting high layout heterogeneity were ultimately screened. Figure 7 illustrates one schematic of the interactive interface. Key functions include: intelligent display of

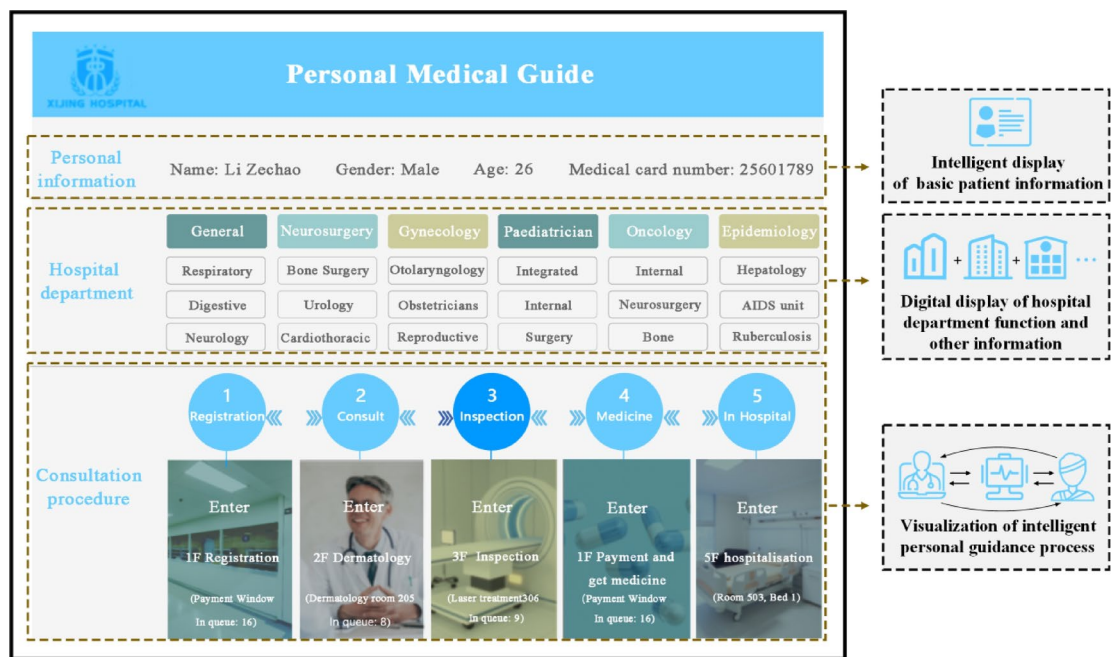


Fig. 7. Interface design sample of intelligent medical guidance desk. (Fig. 7. was obtained from Xijing Hospital, Xi’an, China. In addition, considering the privacy of users, the personal information displayed in the case is computer-generated virtual data.).

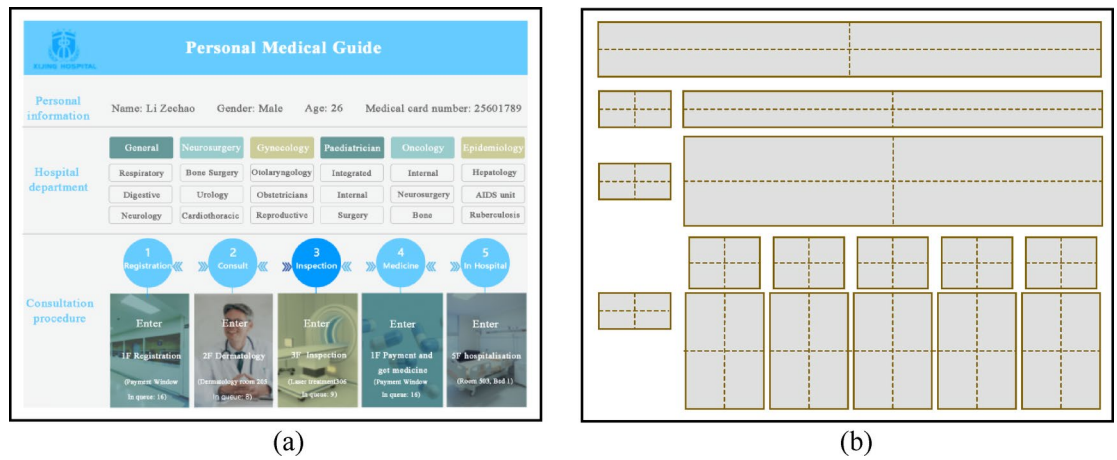


Fig. 8. The abstract representation diagram of the real interface.

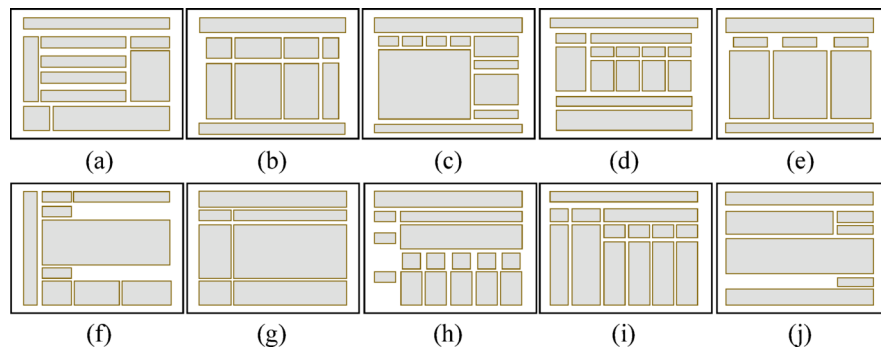


Fig. 9. Abstract rectangular sample schemes.

patients’ basic identity information, digital presentation of hospital department functionalities and information, and—most critically—generating personalized intelligent consultation guidance plans based on physicians’ prescriptions.

Figure 8 illustrates the schematic process of abstracting real interfaces into rectangular layouts. The original interface (Fig. 8-a) is simplified into a minimum bounding rectangle encompassing all internal elements, producing the rectangular layout interface shown in Fig. 8b.

Abstract all real interfaces into rectangular samples schemes, as shown in Fig. 9.

Data source

Aesthetic evaluation values for layout samples were calculated using formulas, while visual cognitive characteristics were measured through eye-tracking experiments. To address potential mismatches between abstract rectangular layouts (Fig. 9) and real interface functionalities, experimental samples were redesigned as shown in Fig. 10. The optimized samples feature a layered design: underlaid with real interfaces and overlaid with semi-transparent abstract rectangular layouts. This hybrid approach ensures participants could intuitively assess rectangular layouts while retaining contextual awareness of the underlying real interfaces during evaluations.

A Latin square design was implemented to counteract order effects, with 20 interface samples randomly divided into 10 pairs (1 abstract semi-transparent image and 1 corresponding real interface image). The experimental phases included: (1) 800 ms central fixation. (2) 5-second free-viewing phase (Fig. 10). (3) Task-oriented phase (locating the radiology icon in the Fig. 7). (4) 800 ms central fixation. All images underwent grayscale conversion (Fig. 11) to minimize color interference.

Figure 12. shows two experimental scenes in which subjects viewed a transparent abstract rectangular stimulus image and a real interface stimulus image.

Let N_i be the i -th intelligent medical guide interface layout scheme, the final initial evaluation data of interface layout aesthetics and visual cognitive are shown in Table 1.

Results and analysis

To Calculate the correlation degree between visual cognitive features and layout aesthetics, a sequence of system characteristic behaviors in terms of gaze duration, gaze count, mean pupil diameter, gaze shift frequency and gaze time percentage for the N_1-N_{10} , denoted by $Y = (Y_1, Y_2, Y_3, Y_4, Y_5)$. Balance, intensity, simplicity,

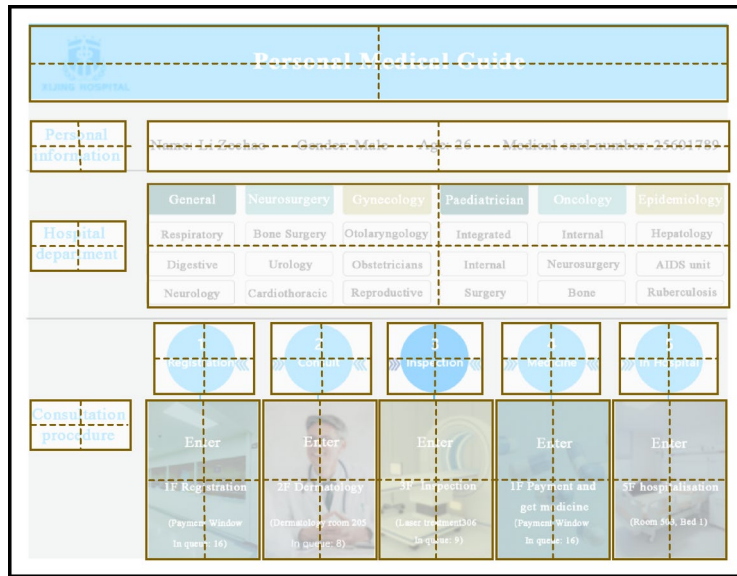


Fig. 10. Transparent abstract rectangular stimulus image schematic diagram.

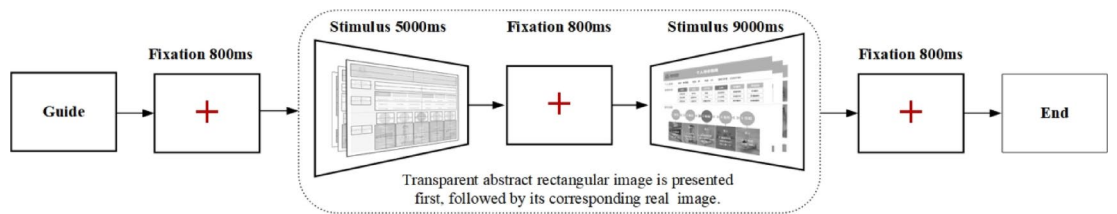


Fig. 11. The process of eye movement experiment.

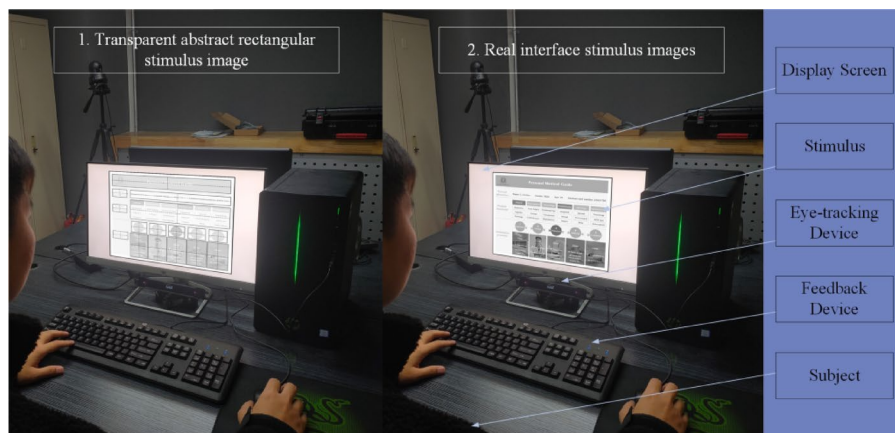


Fig. 12. Experimental scene.

orderliness and uniformity as comparison sequences, denoted by $X = (X_1, X_2, X_3, X_4, X_5)$. First, the data in Table 1 were pre-standardized. Next, comprehensive criterion weights were calculated using Eqs. (1)–(13), with results presented in Table 2. Weighted normalized data outcomes are summarized in Table 3.

Calculate the correlation value between visual cognition and layout aesthetics according to Eqs. (14)–(16), the statistical results are shown in Fig. 13.

(1) Correlation between average pupil diameter and layout aesthetics.

Pearson correlation analysis (data normality confirmed by Shapiro-Wilk test, $p > 0.05$) revealed a negative correlation trend between average pupil diameter and layout aesthetics metrics: $(\hat{R}_H(3, 1) = -0.7404, p < 0.001)$,

Sample	Visual cognitive					Interface layout aesthetics				
	C_1^e	C_2^e	C_3^e	C_4^e	C_5^e	C_1^a	C_2^a	C_3^a	C_4^a	C_5^a
N_1	7535	16.94	4.76	56.30	54.20	0.62	0.77	0.70	0.51	0.66
N_2	4953	11.02	3.18	72.54	76.39	0.88	0.70	0.90	0.89	0.58
N_3	5462	12.36	3.23	66.59	71.22	0.90	0.86	0.62	0.86	0.85
N_4	6872	16.78	4.24	59.46	60.32	0.65	0.78	0.72	0.62	0.67
N_5	4633	8.12	3.00	73.35	80.31	0.90	0.94	0.90	0.92	0.90
N_6	7887	17.43	5.10	50.47	50.26	0.86	0.76	0.77	0.47	0.63
N_7	5942	13.16	3.50	62.10	64.56	0.76	0.76	0.80	0.78	0.78
N_8	8521	20.36	6.20	44.39	46.02	0.51	0.68	0.83	0.35	0.80
N_9	6084	15.48	3.80	60.36	63.18	0.72	0.82	0.76	0.70	0.75
N_{10}	8369	19.25	5.74	45.77	48.85	0.54	0.82	0.65	0.44	0.60

Table 1. The evaluation results of interface layout aesthetics and visual cognitive.

Criteria	Subjective weight	Objective weight	Combination weight	Order
C_1^e	0.0752	0.1229	0.0900	5
C_2^e	0.0933	0.0739	0.0873	8
C_3^e	0.1126	0.0815	0.1029	3
C_4^e	0.0887	0.1028	0.0931	4
C_5^e	0.0806	0.0695	0.0771	10
C_1^a	0.0760	0.1178	0.0890	6
C_2^a	0.0836	0.0887	0.0852	9
C_3^a	0.1313	0.1273	0.1300	2
C_4^a	0.1880	0.0908	0.1577	1
C_5^a	0.0707	0.1250	0.0876	7

Table 2. Combination weights of criteria.

Sample	visual cognitive					layout aesthetics				
	Y_1	Y_2	Y_3	Y_4	Y_5	X_1	X_2	X_3	X_4	X_5
N_1	0.0672	0.0629	0.0566	0.0383	0.0184	0.0251	0.0295	0.0371	0.0443	0.0219
N_2	0.0074	0.0207	0.0058	0.0905	0.0683	0.0844	0.0066	0.1300	0.1494	0.0000
N_3	0.0192	0.0302	0.0074	0.0714	0.0567	0.0890	0.0590	0.0000	0.1411	0.0739
N_4	0.5759	0.0618	0.0399	0.0484	0.0322	0.0319	0.0328	0.0464	0.0747	0.0246
N_5	0.0000	0.0000	0.0000	0.0931	0.0771	0.0890	0.0852	0.1300	0.1577	0.0274
N_6	0.0753	0.0664	0.0675	0.0195	0.0095	0.0799	0.0262	0.0696	0.0332	0.0137
N_7	0.0303	0.4118	0.0161	0.0569	0.0417	0.0571	0.0262	0.0836	0.1190	0.0548
N_8	0.0900	0.0873	0.1029	0.0000	0.0000	0.0000	0.0000	0.0975	0.0000	0.0602
N_9	0.0336	0.0525	0.0257	0.0513	0.0386	0.0479	0.0459	0.0650	0.0968	0.0465
N_{10}	0.0865	0.0794	0.0881	0.0044	0.0064	0.0068	0.0459	0.0139	0.0249	0.0055

Table 3. Standardized weighted evaluation results.

($\hat{R}_H(3, 2) = -0.7380, p < 0.001$), ($\hat{R}_H(3, 3) = -0.3706, p < 0.001$), ($\hat{R}_H(3, 4) = -0.9845, p < 0.001$), ($\hat{R}_H(3, 5) = -0.4910, p < 0.001$). That is, average pupil diameter exhibited the strongest correlation with Orderliness, followed by Balance and Density, with weaker correlations to Unity and Simplicity. The high correlation between Orderliness and average pupil diameter suggests that the logical hierarchy of interface element layouts significantly impacts users' cognitive load. Interface designers should prioritize information hierarchy and guidance cues to reduce cognitive demands and enhance search efficiency. Additionally, Balance demonstrated notable correlation with pupil dynamics, indicating users inherently seek symmetry in horizontal and vertical element distribution. Imbalanced layouts may disrupt visual cognition. Furthermore, Density significantly influenced pupil diameter, implying that excessive elements increase cognitive load.

(2) The correlation between gaze duration and layout aesthetics.

Pearson correlation analysis (data normality confirmed by Shapiro-Wilk test, $p > 0.05$) revealed a negative correlation trend between gaze duration and layout aesthetics metrics: ($\hat{R}_H(1, 1) = -0.6981, p < 0.001$),

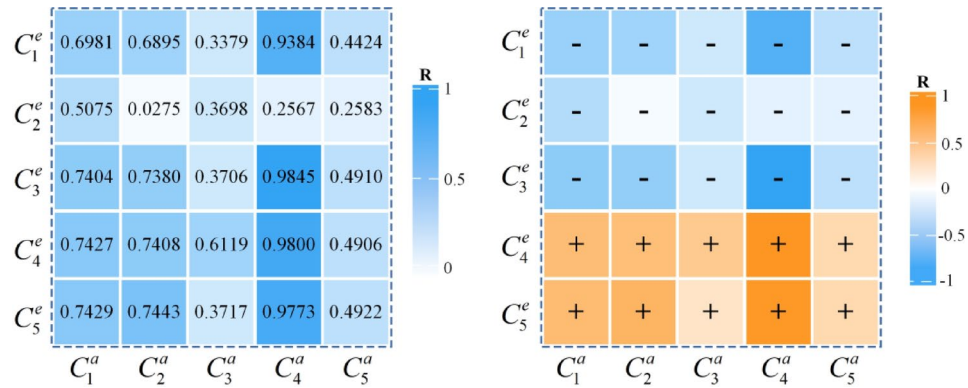


Fig. 13. correlation value(left)and positive and negative correlation(right).

Model Type	MAE	RMSE	Correlation	P-value
Original grey correlation	0.362	0.381	0.6377	< 0.001
New grey absolute correlation	0.271	0.304	-0.3283	0.018
Grey H-convex correlation	0.232	0.322	-0.3523	0.032
Random Forest	0.218	0.296	-0.690	0.008
Our model	0.163	0.237	-0.7404	< 0.001

Table 4. Comparison of model results.

$(\hat{R}_H(1, 2) = -0.6895, p < 0.001)$, $(\hat{R}_H(1, 3) = -0.3379, p < 0.001)$, $(\hat{R}_H(1, 4) = -0.9384, p < 0.001)$, $(\hat{R}_H(1, 5) = -0.4424, p < 0.001)$. It is based on the size of the correlation ordering: $\hat{R}_H(1, 4) > \hat{R}_H(1, 1) > \hat{R}_H(1, 2) > \hat{R}_H(1, 5) > \hat{R}_H(1, 3)$. Correlation analysis revealed that gaze duration exhibited the strongest correlation with Orderliness, followed by Balance and Density, while Uniformity and Simplicity showed the weakest associations.

(3) Correlation between gaze count and layout aesthetics.

Pearson correlation was used after confirming data normality (Shapiro-Wilk test, $p > 0.05$). The correlation results show a negative correlation. $(\hat{R}_H(2, 1) = -0.5075, p < 0.001)$, $(\hat{R}_H(2, 2) = -0.0275, p < 0.001)$, $(\hat{R}_H(2, 3) = -0.3698, p < 0.001)$, $(\hat{R}_H(2, 4) = -0.2567, p < 0.001)$, $(\hat{R}_H(2, 5) = -0.2583, p < 0.001)$. That is, correlation analysis indicates that Balance and Simplicity exhibit the strongest associations with gaze count, followed by Uniformity and Orderliness, while Density shows the weakest correlation. The highest correlation between gaze count and Balance confirms users' heightened sensitivity to interfaces with strong stability and symmetrical equilibrium. Concurrently, the role of Simplicity should not be underestimated: reducing design complexity and variability while maintaining effective information communication is critical for ensuring intuitive usability.

(4) Correlation between gaze shifts frequency and layout aesthetics.

Pearson correlation was used after confirming data normality (Shapiro-Wilk test, $p > 0.05$). The correlation results: $(\hat{R}_H(4, 1) = 0.7427, p < 0.001)$, $(\hat{R}_H(4, 2) = 0.7408, p < 0.001)$, $(\hat{R}_H(4, 3) = 0.6119, p < 0.001)$, $(\hat{R}_H(4, 4) = 0.9800, p < 0.001)$, $(\hat{R}_H(4, 5) = 0.4906, p < 0.001)$. The frequency of gaze shifts demonstrated the strongest correlation with Orderliness, followed by Balance, Density, and Simplicity, while Uniformity exhibited the weakest association.

(5) Correlation between gaze time percentage and layout aesthetics.

Pearson correlation was used after confirming data normality (Shapiro-Wilk test, $p > 0.05$). The correlation is obtained by calculating: $(\hat{R}_H(5, 1) = 0.7429, p < 0.001)$, $(\hat{R}_H(5, 2) = 0.7443, p < 0.001)$, $(\hat{R}_H(5, 3) = 0.3717, p < 0.001)$, $(\hat{R}_H(5, 4) = 0.9773, p < 0.001)$, $(\hat{R}_H(5, 5) = 0.4922, p < 0.001)$. That is, gaze time percentage correlates most strongly with Orderliness, followed by Density and Balance, while Uniformity and Simplicity show the weakest associations.

Discussion

Model validity and performance

(1) Model validity.

To validate the effectiveness of the proposed model, the same data preprocessing methods were employed. Using the average pupil diameter and interface balance as exemplar metrics, we compared the performance of the original grey correlation, new grey absolute correlation, original grey H-convex model and Random Forest across four evaluation criteria: Mean Absolute Error (MAE), Root Mean Square Error (RMSE), correlation, and statistical significance, with aggregated results presented in Table 4.

The proposed comprehensive evaluation framework was systematically compared and demonstrated significant advantages across multiple key performance metrics, as detailed in Table 4. Compared with the

random forest model⁵⁵, Grey H-convex correlation³¹, the improvement of the accuracy of this model comes from the collaborative architecture: the game theory integration of BBWM and M-Critical-RP optimizes the allocation of subjective and objective weights, while the curvature correction term in the H-convex model significantly improves the non-monotonic relationship modeling. Regarding error stability, the proposed model achieved a leading Root Mean Square Error (RMSE) of 0.237, indicating 37.8% lower error fluctuation than conventional grey relational models (RMSE = 0.381), confirming its robustness against outliers. Crucially, correlation analysis revealed a strong negative correlation ($-0.7404, p < 0.001$) in the proposed model, aligning with the observed phenomenon of “enhanced interface symmetry leading to systematic pupil diameter reduction” in eye-tracking experiments. In contrast, the new grey absolute correlation model²² yielded a weaker negative correlation (-0.3283). However, the traditional grey relational model²⁶ produced a counterintuitive positive correlation (0.6377), exposing its theoretical limitations in handling inverse relationships. Statistical validation via Friedman test ($\chi^2=23.17, p < 0.001$) and Nemenyi post-hoc analysis (critical difference $CD = 1.24$) confirmed fundamental performance differences across all benchmarks at $\alpha = 0.05$ significance.

Furthermore, based on the evaluation results from Table 1, line graphs were plotted with interface samples as the X-axis and eye movement and layout aesthetics evaluations as the Y-axis, as illustrated in Fig. 14. Figures 14(a)–14(d) demonstrate that trends in layout aesthetics and visual cognition align closely with the model’s computational outputs.

(2) Model performance.

To validate the model’s performance, BBWM-CRITIC, BWM-CRITIC, and AHP-CRITIC were integrated with the grey H-convex relational model for comparative analysis. The comparative methods were implemented using identical input datasets and standardization protocols, following the same standardized preprocessing procedures as our model. Subjective methods (AHP, BWM) employed the identical expert panel for pairwise indicator comparisons, while objective methods (Entropy, CRITIC) were directly computed from raw data. Additionally, all comparative methods adopted classical implementations without parameter-specific adjustments. The calculation process is as follows: (1) Sample and Data Collection. Data collection involved acquiring layout aesthetic and eye-tracking cognitive data from 50 medical guidance interface prototypes. (2) Calculation of correlation degree. After calculating the comprehensive weight of indicators, the grey H-convex correlation model is used to calculate the correlation degree between X_i and ideal sequence X_0 . (3) Accuracy conversion. Through Receiver Operating Characteristic (ROC) curve analysis, it is determined that when the correlation degree $\hat{R}_H \geq 0.85$, it is an effective scheme. The calculation method of accuracy is:

$$Accuracy = \frac{N(\hat{R}_H \geq 0.85)}{N_{total}} \times 100\% \tag{17}$$

(4) Cross-validation. Divide 50 samples into 5 groups, 10 in each group, and get the overall average accuracy.

Accuracy results across models are illustrated in Fig. 15. The grey H-convex relational model based on the BBWM-M-CRITIC-RP method achieved an overall average accuracy of 88% ($\pm 1.8\%$ SD), followed by BBWM-CRITIC with accuracy above 0.8, while other methods averaged around 0.6. The results indicate that using the BBWM-CRITIC method may increase errors, likely attributable to limitations in CRITIC’s normalization process and linear correlation-based weighting. As sample sizes grow, the accuracy of the AHP-CRITIC method

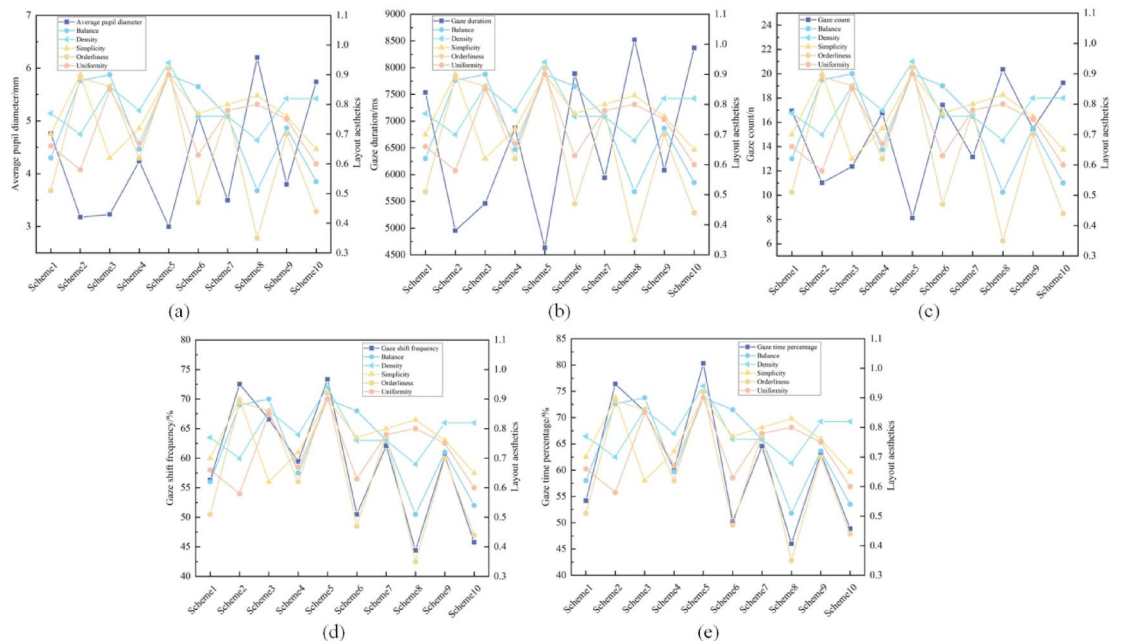


Fig. 14. Visual cognitive features vs. layout aesthetics trend line chart.

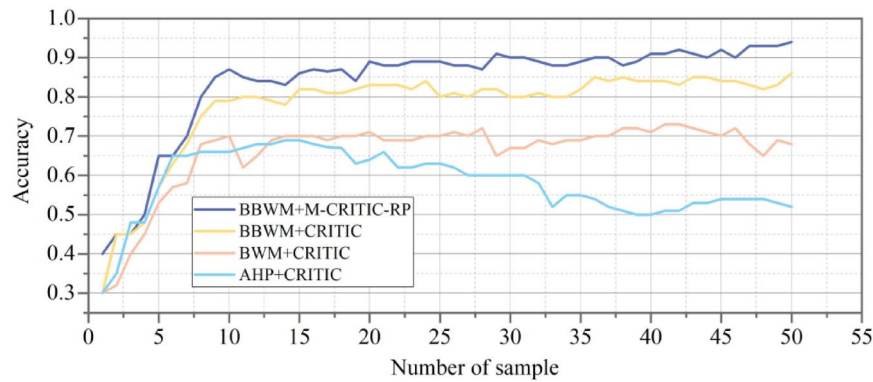


Fig. 15. Comparison of model accuracy.

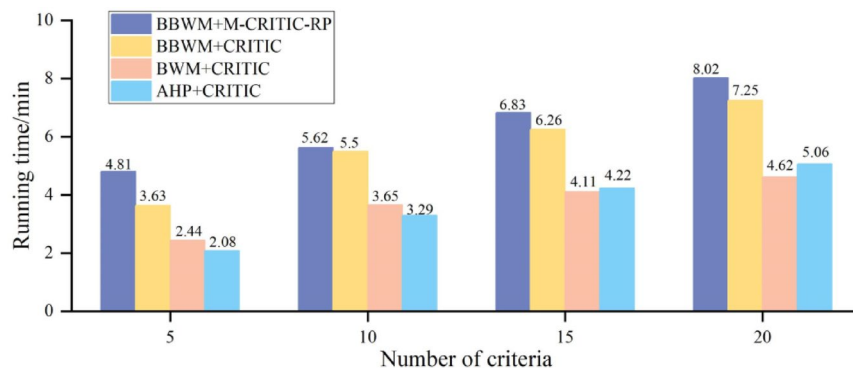


Fig. 16. Comparison of model computation time.

declines below 0.6. This degradation stems from the escalating complexity of pairwise comparisons among criteria, which challenges experts' ability to maintain consistent and precise judgments.

We also evaluated the computation time of the four models. As shown in Fig. 16, under identical sample sizes, the execution time increases with the number of indicators. The BBWM-M-CRITIC-RP method enhances decision-making accuracy but requires the longest computation time due to its complex computational procedures and formulas. In contrast, AHP-CRITIC and BWM-CRITIC involve simpler processes, achieving computation times within 5 min.

Correlation between layout aesthetics and visual cognition

This study reveals the systematic coupling mechanisms between layout aesthetics and visual cognition in medical guidance interfaces through multidimensional correlation analysis. From the perspective of visual information processing theory, the negative correlation between balance and gaze duration ($r = -0.6981$) reflects the profound influence of Gestalt's "law of Prägnanz"⁵⁶ (Ma et al., 2024)—symmetrical spatial distribution of interface elements accelerates the formation of holistic perceptual schemas, thereby reducing cognitive resource consumption in local detail scanning. Additionally, strong negative correlations between density/order and gaze duration ($r = -0.6895$, $r = -0.9384$) provide new theoretical support for attention allocation strategies in visual interface design.

The significant correlation between density and pupil dilation changes ($r = -0.7380$) confirms the "information density threshold effect" in cognitive load theory, where marked pupil expansion indicates cognitive overload compensation, demonstrating isomorphism with the critical inflection phenomenon in interface complexity-efficiency curves⁵⁷. Furthermore, the marked correlations between balance/orderliness and pupil changes ($r = -0.7404$, $r = -0.9845$) establish novel evaluation criteria for applying cognitive load theory to interface design.

The positive reinforcement relationship between order and gaze shift frequency ($r = 0.9800$) elucidates the guiding efficacy of visual hierarchy planning on ocular patterns, aligning with the "visual hierarchy gradient theory" regarding information layering and scanpath matching⁵⁸ (Gomez et al., 2021). The linear correlation between uniformity and gaze time percentage ($r = 0.4922$) confirms that visual coherence optimizes attentional resource allocation by reducing Gestalt closure costs⁵⁹. These findings deepen the mechanistic understanding of aesthetic-cognitive mapping and provide a theoretical foundation for adaptive interface design in smart medical systems through dynamic feedback modeling between layout parameters and cognitive metrics.

Limitations

1) One notable aspect is the complexity of the weight acquisition method, which, to a certain extent, leads to a slight increase in calculation time. Efforts will be directed towards streamlining and simplifying the weight assignment steps in order to mitigate this issue.

2) Interface layout is an important factor affecting cognitive efficiency, but it is also influenced by other factors. For example, the influence of interface style, color, technology and other factors. Future endeavors will center on further addressing the limitations in this research.

3) This study focuses solely on five eye movement metrics, while other metrics (such as gaze path length and gaze hotspot distribution^{60,61}) may also influence interface layout aesthetics. Future research could further explore the potential of additional metrics.

4) While layout aesthetics and visual cognition demonstrate unique advantages for infrequently used medical interfaces, it is noteworthy that other dimensions (e.g., environmental dynamics, cultural symbolism, technological inclusivity) may also influence interface design, constituting a critical research agenda for future investigations.

Conclusion

This article studies the evaluation method of public guidance service interface design based on human aesthetic needs and cognitive characteristics, achieving the evaluation of interface layout aesthetics and measurement of user visual cognitive characteristics, and solving the quantification problem of the mapping relationship between the two. Taking the personal guidance interface of the intelligent medical guidance desk as an example, providing a new method attempt for the evaluation of infrequent contact interfaces.

1) In the theoretical domain of visual display design, this study integrates mathematical modeling and eye-tracking physiological experiments. By employing a more objective quantitative methodology, it elucidates the coupling relationship between interface layouts and human visual cognition. Building upon this foundation, we propose a scientific evaluation method that incorporates users' visual cognitive characteristics, thereby providing methodological references for visual display design. Specifically, we have discovered several interesting phenomena. For public guidance service interfaces, the order has the most significant impact on user visual cognition, with the highest correlation, next is the balance. Density is the most important indicator affecting the fixation count. The impact of uniformity and simplicity on visual cognition is not significant.

2) An improved grey H-convex correlation model was proposed. This study introduces the BBWM and M-CRITIC-RP methods and proposes an improved grey H-convex correlation model to quantify the mapping relationship between user visual cognition and layout aesthetics. By comparing the effectiveness and performance of several existing models, the accuracy of this paper is higher than 88%, which is superior to existing methods.

Data availability

We state that if anyone would like to obtain data from this study, please do not hesitate to contact us. Dr Zhiqiang Wen. bs231011006@sust.edu.cn.

Code availability

<https://github.com/wenzhiqiang28/Algorithm-code>

Received: 20 June 2024; Accepted: 29 April 2025

Published online: 05 May 2025

References

- Pieter, M. A. et al. Demystifying emotion for designers: A five-day course based on seven fundamental principles. *Adv. Des. Res.* **1** (1), 50–62 (2023).
- Wang, P. & Wang, J. Research on the Application of Data Visualization in the UI interface Design of Health Apps, 2021 International Wireless Communications and Mobile Computing (IWCMC), Harbin City, China, 2021, pp. 2013–2019. <https://doi.org/10.1109/IWCMC51323.2021.9498648>
- Peng, H., Liu, S. & Zhang, T. Study on Human-Computer Interaction in the Design of Public Self-service Equipment. In *Advances in Usability, User Experience and Assistive Technology. AHFE 2018. Advances in Intelligent Systems and Computing* Vol. 794 (eds Ahram, T. & Falcão, C.) (Springer,). https://doi.org/10.1007/978-3-319-94947-5_17.
- Rehman, A. U. et al. Development of an intuitive GUI-based fuzzy multi-criteria decision model for comprehensive hospital service quality evaluation and indexing. *Axioms* **12** (10), 921. <https://doi.org/10.3390/axioms12100921> (2023).
- Harvey, G., Bubric, K., VandenBerg, S. & Hair, H. Understanding patient experience in the emergency room using multiple methods. *Des. Health.* **5** (2), 233–251. <https://doi.org/10.1080/24735132.2021.1989133> (2021).
- Rowe, A. & Knox, M. The impact of the healthcare environment on patient experience in the emergency department: a systematic review to understand the implications for patient-centered design. *HERD: Health Environ. Res. Des. J.* **16** (2), 310–329 (2023).
- Sonis, J. D., Aaronson, E. L., Lee, R. Y., Philpotts, L. L. & White, B. A. Emergency department patient experience: A systematic review of the literature. *J. Patient Experience.* **5** (2), 101–106 (2018).
- Melnick, E. R. et al. Back to the bedside: developing a bedside aid for concussion and brain injury decisions in the emergency department. *EGEMS (Wash DC).* **3** (2), 1136. <https://doi.org/10.13063/2327-9214.1136> (2015).
- Hartono, E. & Holsapple, C. W. Website visual design qualities: A threefold framework. *ACM Trans. Manage. Inform. Syst. (TMIS).* **10** (1), 1–21 (2019).
- Baumgarten, A. G. *Aesthetica. Impens* (Ioannis Christiani Kleyb, 1763).
- Sulikowski, P., Kucznerowicz, M., Bąk, I., Romanowski, A. & Zdziebko, T. Online store aesthetics impact efficacy of product recommendations and highlighting. *Sensors* **22** (23), 9186. <https://doi.org/10.3390/s22239186> (2022).
- Fitts, P. M. The information capacity of the human motor system in controlling the amplitude of movement. *J. Exp. Psychol.* **47** (6), 381 (1954).
- Lee, J. D., Wickens, C. D., Liu, Y. & Boyle, L. N. (2017). Designing for people. ShangHai.

14. Lidwell, W., Holden, K. & Butler, J. *Universal Principles of Design, Revised and Updated: 125 Ways To Enhance Usability, Influence Perception, Increase Appeal, Make Better Design Decisions, and Teach Through Design* (Rockport Pub, 2010).
15. Horbinski, T., Cybulski, P. & Medynska, G. Graphic design and button placement for mobile map applications[J]. *Cartographic J.* **57** (3), 196–208 (2020).
16. Niraj, R. D. et al. Interactive layout transfer[J]. *International Conference on Intelligent User Interfaces*, 6(3): 70–80. (2021).
17. Yunsikcho, J. Production of mobile english Language teaching application based on text interface using deep learning[J]. *Electronics* **10** (1809), 2–14 (2022).
18. Lazard, A. & King, A. Objective design to subjective evaluations: connecting visual complexity to aesthetic and usability assessments of ehealth[J]. *Int. J. Human–Computer Interact.* **36** (1), 1–10 (2020).
19. Chen, D. K. et al. An ergonomic design method of manned cabin driven by human operation performance. *Adv. Des. Res.* **1** (Issue 1), 12–20 (2023).
20. Pengnate, S., Sarathy, R. & Kyulee, J. The engagement of website initial aesthetic impressions: an experimental investigation[J]. *Int. J. Human–Computer Interact.* **35** (16), 1517–1531 (2018).
21. Birkhoff, G. D. *Aesthetic measure[M]* (Harvard University Press, 1933).
22. Ngo, D. C. L., Lian, S. T. & Byrne, J. G. Modelling interface aesthetics[J]. *Inf. Sci.* **152** (8), 25–46 (2003).
23. Zyan, F. Z. et al. Research on the influence of user and graphic-Text combined icon construal level fitting on visual cognition[J]. *Appl. Sci.* **7** (12), 1–16 (2022).
24. Zhi, J. Y., Du, Y. & Feng, S. Review on the graphic design and perceptual characteristics of automobile system interface[J]. *Packaging Eng.* **41** (10), 62–70 (2020).
25. Martinez, M. D. et al. Application of eye tracking technology in aviation, maritime, and construction industries: A systematic Review[J]. *Sens. (Basel Switzerland)*, (13):4289. (2021).
26. Deng, J. L. *The Elements of Grey system[M]*63–170 (Press of Huazhong University of Science and Technology, 2002).
27. Zhang, Q. S., Guo, X. J. & Deng, J. L. Grey relation entropy method of grey relation analysis[J]. *Syst. Eng. - Theory&Practice.* **16** (8), 7–11 (1996).
28. Wang, Q. Y. The grey relational analysis of B-Mode[J]. *J. Huazhong Univ. Science&Technology.* **16** (6), 77–82 (1989).
29. Liu, Y., Liu, F. & Forrest, J. A new grey absolute degree of grey incidence model and application[J]. *Chin. J. Manage. Sci.* **20** (5), 173–177 (2012).
30. Wu, L. F., Wang, Y. N. & Liu, S. F. Grey convex relation and its properties[J]. *Syst. Engineering-Theory Pract.* **32** (7), 1501–1505 (2012).
31. Pan, P. G., Chen, Y. M. & Xie, H. Y. Study on Drey H-convex correlation degree model[J]. *Stat. Decis.*, (9): 31–34. (2016).
32. Dang, Y. G. et al. Grey vector modulus incidence model based on panel data and its application[J]. *Control Decis.* ,1–9[2024-01-08] <https://doi.org/10.13195/j.kzyjc.2023.1020>
33. Liu, X. et al. Human reliability evaluation based on objective and subjective comprehensive method used for ergonomic interface design[J]. *Math. Probl. Eng.*, (7): 1–16. (2021).
34. Vrtagić, S. et al. Ranking road sections based on MCDM model: new improved fuzzy SWARA (IMF SWARA). *Axioms* **10** (2), 92 (2021).
35. Gul, M. & Yucesan, M. Performance evaluation of Turkish universities by an integrated bayesian BWM-TOPSIS model. *Socio-Economic Plann. Sci.* **80**, 101173 (2022).
36. Chen, Z. et al. A novel integrated MADM method for design concept evaluation[J]. *Scientific Rep.* **12** (15885), 1–19 (2022).
37. Sharkasi, N. & Saeid, R. A modified CRITIC with a reference point based on fuzzy logic and hamming distance[J]. *Knowl. Based Syst.* **255** (109728), 1–19 (2022).
38. Chen, W. & Hao, X. An optimal combination determining weights method for power quality fuzzy synthetic evaluation. In *International Workshop on Computer Science for Environmental Engineering and EcoInformatics* (pp. 417–423). Berlin, Heidelberg: Springer Berlin Heidelberg. (2011).
39. Lu, C., Li, L. & Wu, D. Application of combination weighting method to weight calculation in performance evaluation of ICT. In *2015 IEEE 15th International Conference on Advanced Learning Technologies* (pp. 258–259). IEEE. (2015), July.
40. Rezaei, J., Nispeling, T., Sarkis, J. & Tavasszy, L. A supplier selection life cycle approach integrating traditional and environmental criteria using the best worst method. *J. Clean. Prod.* **135**, 577–588 (2016).
41. Muhammet, G., Melih, Y., Muhammet, F. & Ak *Control Measure Prioritization in Fine – Kinney-based Risk Assessment: a Bayesian BWM-Fuzzy VIKOR Combined Approach in an Oil station*[J]2959385 (Environmental Science and Pollution Research, 2022). 4.
42. Sharkasi, N., Nguyen, V. H. C. & Jay, R. Export potential analysis of Vietnamese bottled coconut water by incorporating criteria weights of MCDM into the gravity of trade model[J]. *Sustainability* **15** (11780), 1–26 (2023).
43. Wang, W., Wen, Z., Chen, J., Gu, Y. & Peng, Q. Evaluation method for virtual museum interface integrating layout aesthetics and visual cognitive characteristics based on improved Gray H-Convex correlation model. *Appl. Sci.* **14** (16), 7006. <https://doi.org/10.3390/app14167006> (2024).
44. Mokhtar, E. S., Omar, C., Aziz, N. & A., & *Expert Consensus on Formation of Design Principles for Malay Sign Language Mobile Application Based on Nielsen's and Molich's Design Guidelines* (TEM Journal, 2022).
45. Faul, F., Erdfelder, E., Lang, A. G. & Buchner, A. G-Power 3: A flexible statistical power analysis program for the social, behavioral, and biomedical sciences. *Behav. Res. Methods.* **39** (2), 175–191 (2007).
46. Bakaev, M., Goltsova, E., Khvorostov, V. & Razumnikova, O. Data compression algorithms in analysis of UI layouts visual complexity. In *International Andrei Ershov Memorial Conference on Perspectives of System Informatics* (pp. 167–184). Cham: Springer International Publishing. (2019), July.
47. Shao, J. et al. Experimental study on legibility of typographic information of ventilator interface[J]. *Int. J. Ind. Ergon.* **87** (103249), 1–10 (2022).
48. Modi, N. & Singh, J. Understanding online consumer behavior at e-commerce portals using eye-gaze tracking. *Int. J. Human–Computer Interact.* **39** (4), 721–742 (2023).
49. Shao, J., Wu, J., Tang, W. & Xue, C. How dynamic information layout in GIS interface affects users' search performance: integrating visual motion cognition into map information design. *Behav. Inform. Technol.* **42** (11), 1686–1703 (2023).
50. Lounis, C., Pepsakhovich, V. & Causse, M. Visual scanning strategies in the cockpit are modulated by pilots' expertise: A flight simulator study. *PLoS ONE.* **16** (2), e0247061 (2021).
51. Ikuma, L. et al. A guide Fo rassessing control room operator performance using speed and accuracy,perceived workload,situation awareness,and eye tracking. *J. Loss Prev. Process Ind.* **32** (11), 454–465 (2014).
52. Zhou, A. M. et al. Model of synthetic evaluation on interface stylistic beauty based on moderately standardized of index[J]. *J. Zhejiang Univ. (Engineering Science).* **54** (12), 2273–2284 (2020).
53. Li, Y., Wang, Y., Song, F. & Liu, Y. Assessing gender perception differences in color combinations in digital visual interfaces using eye tracking—the case of HUD. *Int. J. Human–Computer Interact.* **40** (20), 6591–6607 (2024).
54. Wu, Y. N. et al. Site selection decision framework for photovoltaic hydrogen production project using BWM-CRITIC-MABAC: A case study in Zhang jiakou[J]. *J. Clean. Prod.* **324** (11), 1–19 (2021).
55. Tao, L. & Xue, X. An improved random forest model to predict bond strength of FRP-to-concrete. *J. Civil Eng. Manage.* **30** (6), 520–535 (2024).
56. Ma, C., Wang, H., Wu, J. & Xue, C. Applying gestalt similarity to improve visual perception of interface color quantity: an EEG study. *Int. J. Ind. Ergon.* **100**, 103521 (2024).

57. Guo, F., Chen, J., Li, M., Lyu, W. & Zhang, J. Effects of visual complexity on user search behavior and satisfaction: an eye-tracking study of mobile news apps. *Univ. Access Inf. Soc.* **21** (4), 795–808 (2022).
58. Gomez, J., Zhen, Z. & Weiner, K. S. Human visual cortex is organized along two genetically opposed hierarchical gradients with unique developmental and evolutionary origins. *PLoS Biol.*, **17**(7), e3000362. (2019).
59. Mungan, E. Gestalt theory: A revolution put on pause? Prospects for a paradigm shift in the psychological sciences. *New Ideas Psychol.* **71**, 101036 (2023).
60. Diaz, G. J., Parade, M. S., Barton, S. L. & Fajen, B. R. The pickup of visual information about size and location during approach to an obstacle. *PLoS One.* **13** (2), e0192044. <https://doi.org/10.1371/journal.pone.0192044> (2018).
61. Zhang, N., Zhang, J., Jiang, S. & Ge, W. The effects of layout order on interface complexity: an Eye-Tracking study for dashboard design. *Sensors* **24** (18), 5966. <https://doi.org/10.3390/s24185966> (2024).

Acknowledgements

The present work is supported by the Innovation capability support program of Shaanxi (Program No.2023-CX-PT-37); Shaanxi Provincial Natural Science Basic Research Program Project (Program No. 2023-JC-QN-0524).

Author contributions

Weiwei Wang and Zhiqiang Wen primarily contributed to the innovative ideas and research, wrote the manuscript text and conducted data analysis; Zhanmei Hu contributed to the data analysis, the experiment design, the readability of articles; Jian Chen, Yanhui Gu, and Qizhao Peng created all the figures, tables, and conducted data analysis. All authors reviewed the manuscript.

Declarations

Competing interests

The authors declare no competing interests.

Ethics statement

This study was approved by the Human Ethics Committee of Shaanxi University of Science and Technology and conducted in the Science Laboratory, School of Design and Art, Shaanxi University of Science and Technology. The experiments were performed according to the Helsinki Declaration. All participants volunteered to participate in this study and gave informed consent before starting the experiment.

Additional information

Correspondence and requests for materials should be addressed to W.W.

Reprints and permissions information is available at www.nature.com/reprints.

Publisher's note Springer Nature remains neutral with regard to jurisdictional claims in published maps and institutional affiliations.

Open Access This article is licensed under a Creative Commons Attribution-NonCommercial-NoDerivatives 4.0 International License, which permits any non-commercial use, sharing, distribution and reproduction in any medium or format, as long as you give appropriate credit to the original author(s) and the source, provide a link to the Creative Commons licence, and indicate if you modified the licensed material. You do not have permission under this licence to share adapted material derived from this article or parts of it. The images or other third party material in this article are included in the article's Creative Commons licence, unless indicated otherwise in a credit line to the material. If material is not included in the article's Creative Commons licence and your intended use is not permitted by statutory regulation or exceeds the permitted use, you will need to obtain permission directly from the copyright holder. To view a copy of this licence, visit <http://creativecommons.org/licenses/by-nc-nd/4.0/>.

© The Author(s) 2025